

Lesion Image Generation Using Conditional GAN for Metastatic Liver Cancer Detection

Yusuke Ikeda, Keisuke Doman, and Yoshito Mekada
Graduate School of Engineering, Chukyo University, Japan
Email: {ikeday, kdoman, y-mekada}@sist.chukyo-u.ac.jp

Shigeru Nawano
International University of Health and Welfare Mita Hospital, Japan
Email: snawano@iuhw.ac.jp

Abstract—In the diagnosis of the abdomen, CT images taken under various conditions are visually checked by multiple doctors. Since diagnosing CT images requires doctors to take time and effort, a Computer-Aided Diagnosis system (CAD) based on a machine learning technique is expected. It is, however, difficult to collect a large number of case images for machine learning. In this paper, we propose a method to generate lesion images by a Conditional Generative Adversarial Networks (CGAN) and show the effectiveness of the proposed method by the accuracy of liver cancer detection from CT images. A CGAN which generates pseudo lesion images is trained with real lesion images labeled with “edge” and “non-edge” of the liver. We confirmed that the proposed method achieved the detection rate of 0.85 and the false positives per case of 0.20. The detection accuracy was higher than that of a conventional method.

Index Terms—CT image, deep learning, computer aided diagnosis, image synthesis

I. INTRODUCTION

The diagnosis for liver cancer is visually performed by doctors with CT images. Interpretation support using machine learning is required to reduce the burden on doctors. However, it is difficult to collect a large number of case images used for machine learning. Thus, we study a method for generating lesion images.

So far, we have constructed a liver cancer detector with a Convolutional Neural Network (CNN). In addition, the lack of learning samples for the detector was compensated by lesion images generated by using three methods including DCGAN. In general, it is difficult to generate a various appearances of lesion images using DCGAN if the learning samples contain different image appearances. Thus, far we have constructed a liver cancer detector with a Convolutional Neural Network (CNN). In addition, the lack of learning samples for the detector was compensated by lesion images generated by using three methods including DCGAN. In general, it is difficult to

generate a new image using DCGAN if the learning samples contain different image appearances.

In this paper, we propose lesion image generation using Conditional GAN (CGAN) that learn lesions with different features separately by using label information in order to suppress the generation of unnatural lesion images while maintaining the variety of lesions that can be represented by DCGAN.

II. RELATED WORK

This chapter describes related work. In recent years, methods using deep learning in general object recognition have reported high detection accuracy. In particular, models such as VGG [1], ResNet [2] using CNN have high detection accuracy, but the amount of training data required for learning is huge. When deep learning is used in the field of medical image processing, it is necessary to add teacher labels to lesions, etc. and use them as learning samples. However, this labeling requires specialized knowledge and it is difficult to prepare medical images. There is data extension as a method of learning with a small amount of data.

Data augmentation methods include Random Erasing [3], cutout [4], mixup [5], etc. In addition, data generation using GAN [6] has been attracting attention as a data extension method using deep learning. GAN has two models, a generator that generates artificial images and a discriminator that distinguishes artificial images from real images. By learning to compete these two models, the generator learns the features of the real image and generates high quality images. DCGAN [7] has also been proposed in which a convolutional layer is added to the GAN model to stabilize learning.

In the rest of this section, we describe the method of generating lesion images and the method of lesion detection using the generated lesions.

A. Lesion Image Generation

It is difficult to collect as many lesion images with various appearances as necessary for machine learning. In deep learning, it is necessary to prepare a sufficient number of learning images, so it is more difficult when targeting rare diseases such as cancer. We proposed three

kinds of methods for generating lesion images of liver cancer as follows.

M1: Synthetic lesion image using Poisson Blending [8]

M2: Lesion images based on CT value distribution [9]

M3: Deep Convolutional Generative Adversarial Networks (DCGAN) [7], [10]

M1 is a method of generating a new 3D image of the lesion by synthesizing a lesion image in the liver of another image by Poisson blending. M2 generates a similar low CT value 3D region by the following function:

$$g(\mathbf{p}) = f(\mathbf{p}) - \frac{k}{1 + \exp(r - n(r))} h(\mathbf{p}) \quad (1)$$

$$n(r) = r_0 + N(0, \sigma_1^2) \quad (2)$$

$$h(\mathbf{p}) = \lambda + N(0, \sigma_2^2) \quad (3)$$

where $\mathbf{p} = (x, y, z)$ is the center coordinates of a shadow (foreground) region, and $g(\mathbf{p})$ is the output CT value at \mathbf{p} . $f(\mathbf{p})$ is the original CT value at \mathbf{p} , and k is a parameter for controlling the contrast between the foreground and the background, and r is the distance between r and the center of the synthesized lesion. $N(0, \sigma^2)$ is a random value following a normal distribution with zero mean and a standard deviation σ .

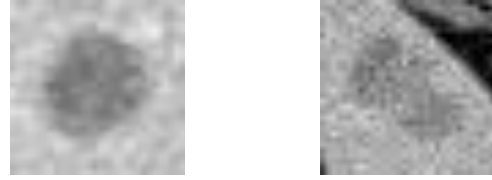
M3 uses DCGAN to generate lesion images. We used 3D images of 110 lesions to generate 3D images. The cross-sections of the 110 3D images were also used to generate 2D images. We showed that the accuracy of lesion detection by CNN, which will be described later, can be improved by adding the lesion images generated by them to the learning image [11]. Table I shows the detection rate and the False Positives (FP) rate per case when lesion images generated by M1, M2, and M3 are used as learning samples of the detector. From the detection results, when the generated lesions of the three methods were used, the detection rate was highest and the false positives per case was low. However, the lesion image generated by DCGAN has a problem of generating the image as shown in Fig. 1. As shown in Fig. 2(b), when the lesion is in the peripheral area of the liver, a linear shadow with a high CT value is observed around the lesion due to the diaphragm, peritoneum, and liver parenchyma. However, the image generated by the DCGANs in Fig. 1 appears to be touching the margin of the liver. Therefore, it is necessary to suppress the generation of images with features that do not exist in real lesions or to select generated lesions so that they are not used for learning samples.

TABLE I. DETECTION RESULTS OF CONVENTIONAL RESEARCH

Method	Detection rate	FP per case
None	0.65	1.80
M1+M2+M3	0.80	0.25



Figure 1. DCGAN generated images with features not found in real lesion.



(a) Non-edge (b) Edge

Figure 2. Cross-section of real lesion image of edge and non-edge.

B. Liver Cancer Detector

Fig. 3 shows the processing flow of the liver cancer detector in the conventional method [12]. This method uses 2D-CNN and 3D-CNN sequentially. Each CNN is based on VGG and uses the artificially generated lesion images described in 2.1 as learning samples in addition to the real lesion images. 2D-CNN scans the axial CT image by raster scan and obtains lesion area candidates. After that, candidate regions are integrated three-dimensionally by the Mean Shift method [10], [13]. The integrated region is identified using 3D-CNN to get the final lesion candidates.

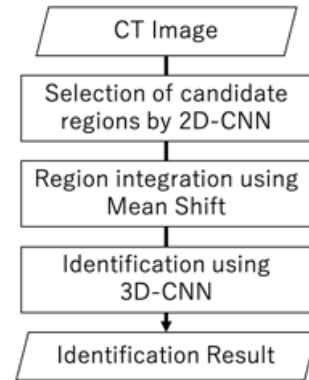


Figure 3. Flow of detector processing.

III. PROPOSED METHOD

Metastatic liver cancer lesions inside the liver (non-edge) and the lesions in the surrounding area (edge) have a very different appearance (Fig. 2). The lesion located inside of the liver is adjacent to the liver parenchyma with uniform CT values and blood vessels with high CT values. On the other hand, the appearance of lesions in the peripheral part of the liver is diverse. Lesions that occur near the lung include the lung region with a low CT value. In addition, fat, other organs, muscles, and ribs that can have various CT values due to contrast effects may be included in the neighbor of the lesion. Therefore, CGAN, which can generate images with different labels, can generate more realistic lesion images. The learning samples dataset uses the portal phase abdominal CT images distributed at the Japan Society for Medical Image Engineering CAD contest. The learning samples for 2D-CNN and 2D-CGAN is obtained by manually selected lesion image with 32×32 pixels, and the learning samples of 3D-CNN and 3D-CGAN is obtained by the same way with $32 \times 32 \times 20$ voxels.

IV. EXPERIMENTS

In order to evaluate the effectiveness of the lesion image generated by CGAN, the generated image was used as learning samples for the detector. Twenty CT images that were not used for CGAN and CNN learning samples were used as evaluation data. The proposed method was evaluated using the detection rate and the false positives rate per case. In this paper, the detection target disease is metastatic liver cancer of 20mm or less.

A. CGAN Learning Samples

The lesion images used for 2D-CGAN learning are shown in Table II, and the lesion images used for 3D-CGAN learning are shown in Table III. "Rotation, etc." in these tables represent data augmentation based on geometric deformation. In 3D-CGAN learning samples, learning does not converge because the number of real lesion images is not sufficient. Thus, as in the reference [3], synthesis images generated by M1 and M2 also use as learning samples for the CGAN.

TABLE II. 2D-CGAN LEARNING SAMPLES

Label	Real	Rotation etc.
Edge	255	1785
Non-edge	482	3374

TABLE III. 3D-CGAN LEARNING SAMPLES

Label	Real	Rotation etc.	M1	M2
Edge	26	390	6087	5072
Non-edge	84	1260	4554	5926

Fig. 4 shows lesion images learned under these conditions. These generated lesion images are used as learning samples for the detector.

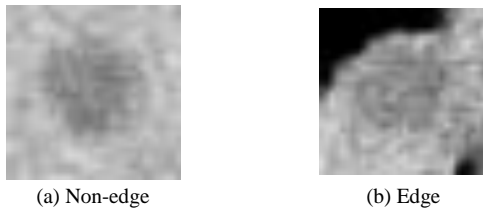


Figure 4. Cross-section of lesion image generated by CGAN.

B. Detector Learning Samples

Table IV shows the number of real lesions among the data used for detector learning, and Table V shows the number of data generated by DCGAN or CGAN.

TABLE IV. LEARNING SAMPLES COMMON TO DETECTORS

Model	Real	M1	M2	Negative
2D	737	3,000	3,000	4,500
3D	110	1,000	1,000	1,500

TABLE V. DIFFERENT LEARNING SAMPLES FOR EACH METHOD

Method	Model	DCGAN	CGAN	
			Edge	Non-Edge
Conventional	2D	3,000	0	0
	3D	1,000	0	0
CGAN Edge	2D	0	3,000	0
	3D	0	1,000	0

CGAN Non-Edge	2D	0	0	3,000
	3D	0	0	1,000
CGAN	2D	0	1,500	1,500
	3D	0	500	500

C. Detection Results

Detection results for 20 evaluation CT images are shown in Table VI. Compared with the conventional method, the detection rate increased and the false positives rate per case decreased when both the edge and non-edge lesions generated by CGAN were used for learning. This confirmed the effectiveness of the proposed method.

TABLE VI. DETECTOR RESULT

Method	Detection rate	FP per case
Conventional	0.80	0.25
CGAN edge	0.85	0.35
CGAN non-edge	0.75	0.20
CGAN	0.85	0.20

D. Discussion

The highest detection accuracy and low false positives per case were achieved by simultaneously using the lesion images at the edge of the liver generated by CGAN and the lesion images located inside the liver. As shown in Fig. 5, the lesions near the edge of the liver were detected correctly. However, as shown in Fig. 6, it was not possible to detect small lesions or lesions with small contrast with the surrounding area. Fig. 7 shows an example of false positive case. False positives occurred in areas where the liver was recessed or outside the liver. Fig. 8 shows an example of a lesion located at the edge of the liver that could not be detected by the conventional method. Although it is necessary to continue to investigate how many lesion images are appropriate to generate, it is effective to generate images of lesions inside the liver and lesions at the edge of the liver separately and to use them as learning samples has been confirmed.

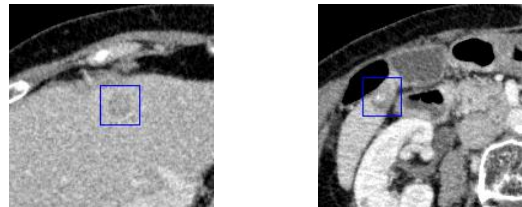


Figure 5. Examples of detected lesions.

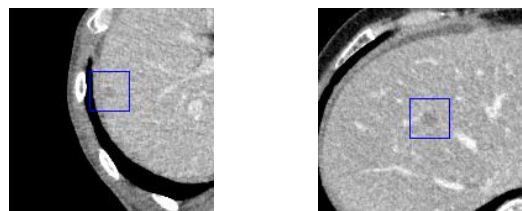


Figure 6. Examples of undetected lesions.

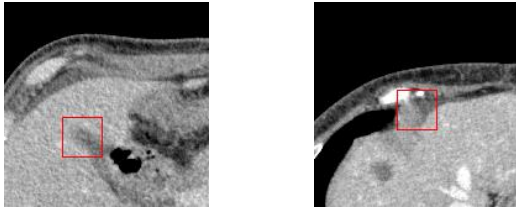


Figure 7. Examples of false detected lesions.



Figure 8. The lesion not detected by conventional methods.

V. CONCLUSION

We proposed a lesion generation method using CGAN as a method to generate a large number of learning samples for machine learning. Since the appearance of liver cancer differs depending on the location where it occurs, more realistic lesion images could be generated by conditional GAN. The detection accuracy is improved compared to the lesion generation method using DCGAN by generating each separately with CGAN and using it as learning samples for the detector. However, the evaluation was not sufficient because there were only 20 cases used for evaluation. Thus, it is necessary to conduct large-scale evaluation experiments in the future.

CONFLICT OF INTEREST

The authors declare no conflict of interest.

AUTHOR CONTRIBUTIONS

Yusuke Ikeda conducted the research and wrote the paper; Yoshito Mekada and Keisuke Doman reviewed and edited the paper; Shigeru Nawano provided the data to use for the research; all authors had approved the final version.

ACKNOWLEDGMENT

Part of this research is supported by grants from the Japan Society for the Promotion of Science.

REFERENCES

- [1] K. Simonyan and A. Zisserman, "Very deep convolutional networks for large-scale image recognition," in *Proc. International Conference on Learning Representations*, May 2015.
- [2] S. Targ, D. Almeida, and K. Lyman, "Resnet in resnet: Generalizing residual architectures," in *Proc. International Conference on Learning Representations*, May 2016.
- [3] Z. Zhong, L. Zheng, G. Kang, S. Li, and Y. Yang. (Nov. 2017). Random erasing data augmentation. arXiv. [Online]. Available: <https://arxiv.org/pdf/1708.04896.pdf>
- [4] T. DeVries and W. G. Taylor. (Nov. 2017). Improved regularization of convolutional neural networks with cutout. arXiv. [Online]. Available: <https://arxiv.org/pdf/1708.04552.pdf>

- [5] H. Zhang, M. Cisse, Y. N. Dauphin, and D. Lopez-Paz, "Mixup: Beyond empirical risk minimization," in *Proc. International Conference on Learning Representations*, May 2018.
- [6] I. J. Goodfellow, J. Pouget-Abadie, M. Mirza, B. Xu, D. Warde-Farley, S. Ozair, A. Courville, and Y. Bengio, "Generative adversarial nets," *The advances in Neural Information Processing Systems*, pp. 2672-2680, Dec. 2014.
- [7] A. Radford, L. Metz, and S. Chintala, "Unsupervised representation learning with deep convolutional generative adversarial networks," in *Proc. International Conference on Learning Representations*, May 2016.
- [8] P. Perez, M. Gangnet, and A. Blake, "Poisson image editing," *ACM Special Interest Group on Computer*, vol. 22, no. 3, pp. 313-318, July 2003.
- [9] T. Konishi, K. Doman, Y. Mekada, and S. Nawano, "Metastatic liver cancer detection by CNN using artificial lesion images," *Medical Imaging Technology*, vol. 37, no. 1, pp. 46-50, Jan. 2019 (in Japanese).
- [10] T. Konishi, K. Doman, Y. Mekada, and S. Nawano, "Lesion image synthesis using DCGANs for metastatic liver cancer detection," in *Proc. International Workshop on Frontiers of Computer Vision*, Feb. 2018.
- [11] M. Mirza and S. Osindero. (Nov 2014). Conditional generative adversarial nets. arXiv. [Online]. Available: <https://arxiv.org/pdf/1411.1784.pdf>
- [12] T. Konishi, K. Doman, Y. Mekada, and S. Nawano, "Metastatic liver cancer detection by 3D-CNN using artificial lesion images," *IEICE Technical Committee on Medical Imaging Technical Research Report*, vol. 116, no. 393, pp. 21-22, Jan. 2017 (in Japanese).
- [13] Y. Cheng, "Mean shift, mode seeking, and clustering," *IEEE Trans. on Pattern Analysis and Machine Intelligence*, vol. 17, no. 8, pp. 790-799, Aug. 1995.

Copyright © 2021 by the authors. This is an open access article distributed under the Creative Commons Attribution License ([CC BY-NC-ND 4.0](https://creativecommons.org/licenses/by-nc-nd/4.0/)), which permits use, distribution and reproduction in any medium, provided that the article is properly cited, the use is non-commercial and no modifications or adaptations are made.

Yusuke Ikeda received his B.S degree in engineering at the Chukyo University, Japan in 2019. He is currently studying for M.S degree in engineering at the Chukyo University in Japan. His research is mainly the analysis of medical images using machine learning.

Keisuke Doman received his B.S. degree from the Department of Electrical and Electronic Engineering, his M.S. degree and Ph.D. from the Graduate School of Information Science at Nagoya University in 2007, 2009, and 2012, respectively. He is currently an Associate Professor at the School of Engineering, Chukyo University, Japan. His current re-search interests include the application of computer vision and pattern recognition to human activity support systems. He is a member of IEICE, IEEE, ACM, and INSTICC.

Yoshito Mekada received the B.S., M.S., and Ph.D. degrees in information engineering from Nagoya University, Japan in 1991, 1993, and 1996, respectively. He is currently a professor at the School of Engineering, Chukyo University, Japan. His current research interests include medical image recognition, computer vision, and their applications. He is a member of the Japanese Society of Medical Imaging Technology and the IEEE.

Shigeru Nawano graduated from the School of Medicine, Chiba University, in 1981. He became a research associate at Chiba University Hospital in 1982. He moved to the Diagnostic Radiology Division, National Cancer Center Hospital, in 1986, where he was chief of the Radiology Division, National Cancer Center Hospital East. Since 2007, he joined International University of Health and Welfare, where he is a professor. His research activities include computed radiography, mammography, MRI, CT and computer-aided diagnosis. He is the member of Japan Radiological Society, the Japanese Society of Nuclear Medicine and the Japanese Society of Medical Imaging Technology. He holds M.D./Ph.D. degrees.